

HEAT DISSIPATION MECHANISM OF NARROW GAP VERTICAL CHANNELS WITH POROUS MEDIA

*Yanhong LU^{*1}, Hui LI¹, Jing LIU¹, Lingtao WENG²*

^{*1}School of Mechanical and Electrical Engineering and Automation, Tianjin Vocational Institute, Tianjin 300410, China

²Key Laboratory of Mechanism Theory and Equipment Design of Ministry of Education, Tianjin University, Tianjin 300354, China

* Corresponding author; E-mail: luyanhong80@126.com

This study mathematically employs theoretical deduction methods to solve the analytic solutions of velocity and temperature. It also investigates the effect of the aspect ratio of the narrow gap vertical channel filled with porous media and porosity through simulation. Particularly, to clearly explore the comprehensive influence law of these parameters, we extensively discussed quantitative relationship by fitting between flow resistance, heat transfer coefficient, exergy and channel aspect ratio, porosity, Reynolds number based on equivalent diameter. The relative errors between simulation and fitting results about f and Nusselt number are almost within $\pm 10\%$. For this study, the exergy critical Reynolds number is 2147.5. When aspect ratio is 0.1, the convective heat transfer coefficient reaches its maximum. Besides, to verify correctness of the calculation and simulation, we built the experimental platform and measured temperature and velocity in narrow gap vertical channel filling copper foam with different porosity. The uniqueness of this study lies in resolving the heat dissipation mechanism of the narrow gap vertical channel filled with porous media, which has not been attempted before. This work provides insights into the flow and heat transfer mechanism of such channels and helps improve the performance and lifespan of high-power electronic devices.

Key words: Porous media; Narrow gap vertical channel; Heat dissipation mechanism; Exergy analyses

1. Introduction

The long-term operation of high-power electronic devices can lead to severe local heating, resulting in performance degradation or shortened lifespan. In severe cases, fires. Therefore, we should ensure a uniform temperature distribution and rapid heat dissipation. Most of these devices are narrow gap vertical channels, for example, electric vehicle battery packs.

Open porous media has the character of a high specific surface area and can solve the problem of uneven temperature distribution [1-3]. For example, it has been proven that porous media plate channel can enhance heat transfer. Mahmoudi [4] and Ouyang [5] proved this by solving the momentum equation and energy equation different thermal boundary conditions. Dehghand [6-8]

solved the heat dissipation mechanism of porous media by using perturbation theory. To illustrate heat dissipation effect of porous media filled into different channel, some [9-12] analyzed the effect of heat transfer in the circular porous pipe by numerical analysis. Attention has also been paid to rectangular or special-shaped channel. Bahmani [13] and Kurtbas [14-16] studied influencing factors of the flow and heat transfer of porous channel of rectangular or square size vanes. Chen [17] and Huisseune [18] studied heat exchangers with porous. Jalili [19] and Ahmadi Azar [20] investigated MHD fluid flow and heat transfer through the porous medium wavy or wedge channel by analytical and numerical study.

It is worth noting that most of the studies above have been conducted that porous media can make temperature distribution more uniform and heat dissipation faster in flat channels, circular channels, or rectangular channels. However, effect of channel shape and size parameters has not been studied clearly, in particular in narrow gap vertical channel filling the porous media (NGVCP) which is common in high heat production devices, such as high power electronic devices, power batteries, etc.

The current study aims to investigate the effects mechanism of aspect ratio of narrow gap channels, porosity, and Re number based on hydraulic radius on flow and heat transfer processes of NGVCP by theoretical derivation, numerical simulation, equation fitting and experimental verification.

2. Heat transfer mechanism in porous media

Based on the Brinkman-Darcy extended model and the local non-thermal equilibrium heat transfer model, it is assumed that the pores of porous media are uniform and isotropic. The velocity and temperature fields in the channel are fully developed. Neglecting the thermal conduction effect in the fluid flow direction, the fluid is in uniform parallel flow and there is no internal heat source [4, 21]. The space between the two plates is $2H$, the plate length is $L(L \gg H)$. Both plates have constant heat flux q_w .

2.1. Analytical solution of flow velocity distribution

The momentum equation of fluid flow through porous media is simplified

$$\mu_e \frac{d^2 u}{dy^2} - \frac{\mu_f}{K} u + B = 0 \quad (1)$$

Here, μ_f is the viscosity of the fluid, and μ_e is the effective dynamic viscosity. Moreover, $\mu_e = \mu_f / \varepsilon$, where ε is porosity. u is the velocity of the fluid. B is the negative value of the axial pressure gradient, $B = -dp/dx$. When $y=H$, $u=0$; When $y=0$, at the center of the channel, $du/dy=0$.

Introduce the following dimensionless numbers [22],

$$M = 1 / \varepsilon, \eta = y / H, U = \mu_f u / B H^2, Da = K / H^2, S = \sqrt{\frac{\varepsilon}{Da}}.$$

Solve the momentum equation, then express it in terms of dimensionless flow velocity.

$$U = Da \left[1 - \frac{\cosh(S\eta)}{\cosh S} \right] \quad (2)$$

$$u^* = U / U_m = \frac{S}{S - t \operatorname{anh} S} \left[1 - \frac{\cosh(S\eta)}{\cosh S} \right] \quad (3)$$

When the porous medium is not filled, $u_c^* = \frac{3}{2}(1 - \eta^2)$.

2.2. Analytical solution of temperature distribution

For porous media, there are both solid and fluid, so their energy equations are

$$0 = k_{se} \frac{\partial^2 T_s}{\partial y^2} - h_{sf} a_{sf} (T_s - T_f) \quad (4a)$$

$$\rho_f C_p u \frac{\partial T_f}{\partial x} = k_{fe} \frac{\partial^2 T_f}{\partial y^2} + h_{af} a_{af} (T_s - T_f) \quad (4b)$$

In the formula, k_{se} and k_{fe} are respectively the effective thermal conductivity of the solid and fluid. T_s and T_f are the temperatures of the solid and fluid respectively. h_{sf} is the surface convective heat transfer coefficient. a_{sf} is the specific surface area. ρ_f is the density of fluid. C_p is the specific heat of fluid at constant pressure.

Introduce the following dimensionless numbers, $k = k_{fe} / k_{se}$; $B = h_{sf} a_{sf} H^2 / k_{se}$. Add the eq.(4a) and (4b), and integrate them on 0-H to obtain the analytical solution of the dimensionless temperature distribution of fluid and solid.

$$\begin{aligned} \theta_f = & \frac{a}{k \cosh \sigma} \left(\frac{b}{S^2 - \sigma^2} + \frac{b}{\sigma^2} - \frac{B}{\sigma^4} \right) \cosh(\sigma\eta) \\ & - \frac{ab}{k \cosh S (S^2 - \sigma^2)} \cosh(S\eta) + \frac{aB}{2k\sigma^2} \eta^2 + \frac{a}{k\sigma^4} \left(B - \sigma^2 b - \frac{1}{2} B \sigma^2 \right) \end{aligned} \quad (5a)$$

$$\theta_s = -\frac{a}{S^2 \cosh S} \cosh(S\eta) + \frac{a}{2} \eta^2 + \frac{a}{2S^2} (2 - S^2) - k\theta_f \quad (5b)$$

Here, $a = \frac{S \cosh S}{S \cosh S - \operatorname{sinh} S}$, $\sigma = \sqrt{\frac{(1+k)B}{k}}$, $b = 1 - B/S^2$.

Without porous media, under the same assumptions,

$$\theta = \frac{1}{8}(6\eta^2 - \eta^4 - 5) \quad (6)$$

2.3. Nusselt number

Introduce the dimensionless temperature and the effective thermal conductivity ratio k into the expression for the average Nu number in a flat channel with porous media,

$$Nu_p = \frac{4}{k \left(-\int_0^1 u^* \theta_f d\eta \right)} \quad (7)$$

Calculate by MATLAB to obtain the Nu number. Nu_p is always greater than the Nu number of empty channel, which is 8.235. To verify the reliability of the theoretical model, the results in this paper compared with that in previous literature [5, 8], and they are in good agreement. That is obviously noted from Fig.1. But, for previous studies, the boundary condition setting and calculation process are complex; research results are discrete data rather than continuous data.

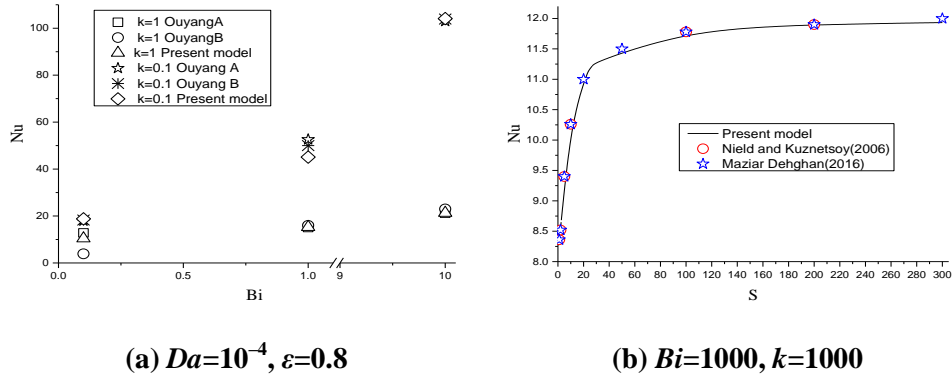


Figure 1. Comparison of Nu number in this article with previous studies

3. Numerical analysis of flow and heat transfer in NGVCP

Based on the theory researches about flow and heat transfer, numerical simulation analysis based the RNG k-e model in NGVCP was conducted. The model size of the heating plates on both sides of NGVCP is $200\text{mm} \times 80\text{mm}$. There is a constant heat flow q on left and right sides of the channel.

3.1. Results and discussion

When the channel width is 4mm and the air inlet velocity is 2.7m/s, read the velocity and temperature at four positions in the flow cross section which is 1mm, 10mm, 20mm, and 50mm from the inlet. In NGVCP, the velocity distribution and temperature distribution pattern is mainly consistent along the length direction, and it is nearly linear. In empty channel, the velocity distribution and temperature distribution are close to the parabola. Corresponding relationships of velocity distribution and temperature distribution of porous channel and empty channel were depicted in Fig.2. That is

consistent with the previous theoretical analysis results. That is mutually verified. Adding porous media in the channel helps reduce boundary layer thickness, enhance turbulence, and make velocity distribution more uniform. This in turn makes the temperature distribution of high power electronic devices uniform and avoids local overheating.

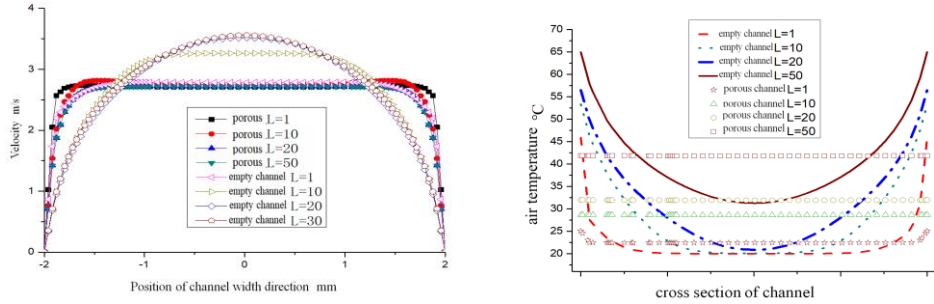


Figure 2. Velocity distribution and temperature distribution of flow cross section

The ratio of channel width to height, that is aspect ratio, is defined as Ω . The height of NGVCP is 80mm. Widths and its corresponding equivalent diameter (Dh) and aspect ratio are shown in Tab.1.

Table 1. The aspect ratio and hydraulic diameter about different channel widths

Width(mm)	2	4	6	8	10	12	14	16
Ω	0.025	0.05	0.075	0.1	0.125	0.15	0.175	0.2
Dh (mm)	3.90	7.62	11.16	14.55	17.78	20.87	23.83	26.67

When the inlet velocity is constant, with the increase of aspect ratio, the Nu number based on equivalent diameter gradually becomes bigger, and the convective heat transfer coefficient first increases and then stabilizes. When the channel width increases to certain, the convective heat transfer coefficient reaches its maximum. When channel width continues to grow and the convective heat transfer coefficient remains unchanged nearly. It is obvious from Fig. 3. For narrow gap rectangular channels, when aspect ratio reaches or exceeds 0.1, the heat dissipation effect is obvious. Porous media have a large specific surface area and extended heat transfer paths, which allows for more efficient removal of heat, leading to a noticeable improvement in heat dissipation effect.

When volume is constant, the cross sectional velocity decreases with the width increasing, so convective heat transfer is weak. It is noted from Fig.4 that Nu number based on the equivalent diameter first increases and then stabilizes. Although the convective heat transfer coefficient decreases, the product of h and the equivalent diameter D_h still increases when Ω is small, and then gradually stabilizes. When the Re_{D_h} is constant, the resistance decreases with the increase of porosity. To achieve low resistance, it is advisable to choose porous media with high porosity 0.9.

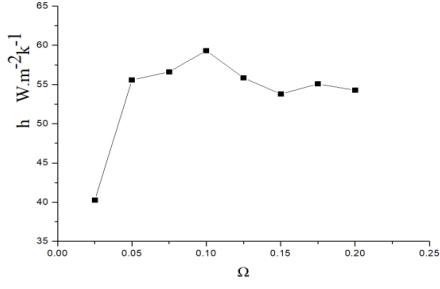


Figure 3. h with Ω at constant velocity

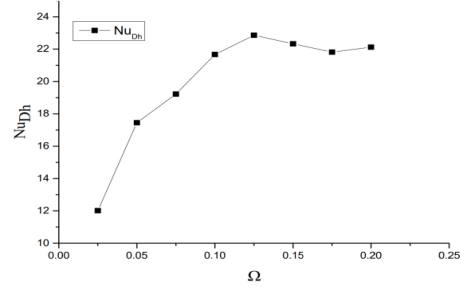


Figure 4. Nu_{Dh} with Ω at constant volume

3.2. Resistance and heat transfer characteristic criterion equation fitting

In order to further investigate the comprehensive effects of aspect ratio and porosity on flow and heat dissipation in NGVCP, the characteristic equations fitting were carried out. For NGVCP, resistance is not only related to Re number, but also has a functional relationship with the porosity. So characteristic equation for flow resistance f is

$$f = C Re_{Dh}^m \varepsilon^n \quad (8)$$

Here, n , C and m are undetermined coefficients. Based on the data under various conditions, the expression for the resistance coefficient f is fitted as

$$f = 63.0196 Re_{Dh}^{-0.3121} \varepsilon^{-3.2749} \quad (9)$$

Comprehensively consider porosity, aspect ratio of the channel and Re number based the equivalent diameter, fit the heat transfer characteristic criterion equation in NGVCP,

$$Nu = 0.0769 Re_{Dh}^{1.1524} \varepsilon^{0.5252} \Omega^{0.9665} \quad (10)$$

The formulas are applicable to $998 < Re_{Dh} < 4006$, $0.6 < \varepsilon < 0.95$, $0.05 < \Omega < 0.2$. For resistance coefficient f , the correct decisive coefficient $AdjR^2$ is 0.9593. For Nu number, $AdjR^2$ is 0.9812. The relative error between simulation and fitting results about f and Nu is almost within $\pm 10\%$ and $\pm 8\%$, respectively, so fitness of the data is high, which can be clearly proved by Fig.5.

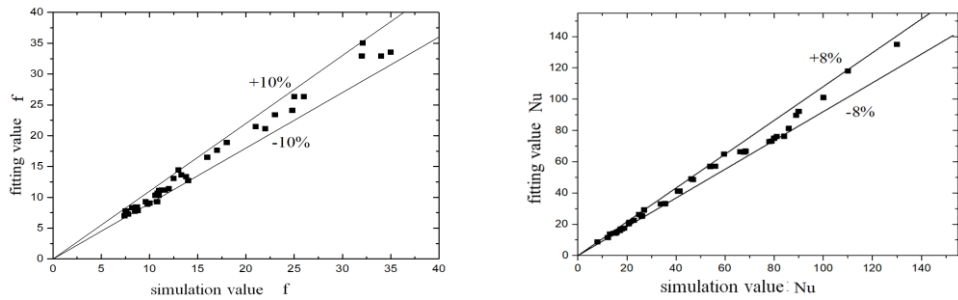


Figure 5. Comparison of simulated and fitted values

3.3. Exergy of convective heat transfer in NGVCP

Assuming that the flow and heat transfer process of the fluid is fully developed, according to the definition of entropy [14], the local convective heat transfer exergy transfer coefficient h_{ex} is

$$h_{ex} = \frac{\rho h D_h u_m}{4q_w} \left[C_p \left(1 - \frac{T_0}{T_{fi} + \frac{4hq_w x}{hD_h \rho u C_p}} \right) \frac{dT_f}{dx} + \frac{\nu T_0}{T_{fi} + \frac{4S_t q_w x}{hD_h}} \frac{dp}{dx} \right] \quad (11)$$

In the formula, T_f is the temperature of the air, K; T_0 is the ambient temperature, K; C_p is constant pressure specific heat capacity, $\text{Jkg}^{-1}\text{K}^{-1}$; ν is the specific volume of the fluid, m^3kg^{-1} . Integrate to come to the average exergy transmission coefficient

$$h_{ex,m} = h \left[1 - \frac{\text{Re}_{D_h} \text{Pr}}{4N_q N_{T_{fi}} N_L} \left(1 + \frac{f \text{Re}_{D_h}^3}{8N_{q_w}} \right) \ln \left(1 + \frac{4N_q N_L}{\text{Re}_{D_h} \text{Pr}} \right) \right] \quad (12)$$

$$\text{Here, } N_q = \frac{q_w D_h}{\lambda T_{fi}}, \quad N_{T_{fi}} = \frac{T_{fi}}{T_0}, \quad N_L = \frac{L}{D_h}, \quad N_{q_w} = \frac{q_w \rho^2 D_h^3}{\mu^3}.$$

Here, q_w is the heat flux, Wm^{-2} . T_{fi} is the temperature of the inlet air, K. μ is the viscosity coefficient of the gas, $\text{kgm}^{-1}\text{s}^{-1}$; L is the length of the channel, m; λ is the thermal conductivity of gas, $\text{Wm}^{-1}\text{K}^{-1}$; h is the heat transfer coefficient, $\text{Wm}^{-2}\text{K}^{-1}$.

The average transmission exergy Nu number is

$$Nu_e = \frac{h_{ex,m} D_h}{\lambda} = Nu_{D_h} \left[1 - \frac{\text{Re}_{D_h} \text{Pr}}{4N_q N_{T_{fi}} N_L} \left(1 + \frac{f \text{Re}_{D_h}^3}{8N_{q_w}} \right) \ln \left(1 + \frac{4N_q N_L}{\text{Re}_{D_h} \text{Pr}} \right) \right] \quad (13)$$

There is a coupling relationship between the velocity field and the temperature field in the convective heat transfer process. The average transfer exergy Nu number is the difference between the exergy obtained during temperature difference heat transfer and the exergy loss caused by the viscous flow of the medium, which is $Nu_e = Nu_{eT} - Nu_{eP}$. Nu_{eT} is the heat transfer exergy Nu number obtained by temperature difference heat transfer, while Nu_{eP} is the heat transfer exergy Nu number by the flow resistance loss. Generally, $Nu_{eT} > Nu_{eP}$. But it is possible that at a certain Re number, Nu_{eT} is less than Nu_{eP} . At this time, the average transfer exergy Nu number is less than 0.

$$Nu_{eT} = Nu_{D_h} \left[1 - \frac{\text{Re}_{D_h} \text{Pr}}{4N_{q_w} N_{T_{fi}} N_L} \ln \left(1 + \frac{4N_q N_L}{\text{Re}_{D_h} \text{Pr}} \right) \right] \quad (14)$$

$$Nu_{ep} = \frac{f Re_{Dh}^4 Nu Pr}{32 N_{qw} N_{Ti} N_L N_{qw}} \ln \left(1 + \frac{4 N_q N_L}{Re_{Dh} Pr} \right) \quad (15)$$

Calculate resistance factor f under different Re_{Dh} numbers through pressure drop, velocity, air density and other parameters. With the increase of the Re_{Dh} number, f falls. The correlation between the f and Re_{Dh} number is $f = a Re_{Dh}^b$. In this study, for NGVCP (foam copper, porosity is 0.9), the fitting curve is $f = 62255 Re_{Dh}^{-1.1}$ and the maximum error between the calculation and the fitting is less than 8%. It is obvious that the error between the calculated values and the fitting is very small, as can be clearly seen from Fig.6. From Fig.7, with the increase of Re_{Dh} number, Nu_{eT} and Nu_{eP} are both going up trends. However, Nu_{eP} increases much faster than Nu_{eT} . When the Re_{Dh} number rises to a certain value, $Nu_{eT} < Nu_{eP}$. When $Nu_{eT} = Nu_{eP}$, namely $Nu_e = 0$, the Re_{Dh} number is called the exergy critical Re number. For this study, the exergy critical Re_{Dh} number is 2147.5. When $Re_{Dh} = 2147.5$, $Nu_{eT} = Nu_{eP} = 2.273$, and $Nu_e = 0$. Average exergy Nu number Nu_e drops with the increase of Re_{Dh} number, because the irreversible thermodynamic process generate.

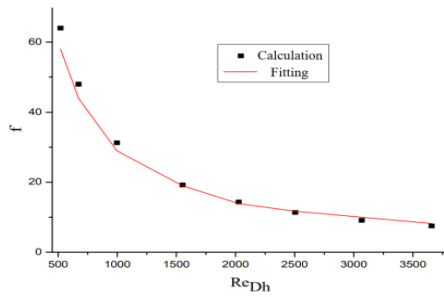


Figure 6. Resistance factor f with Re_{Dh}

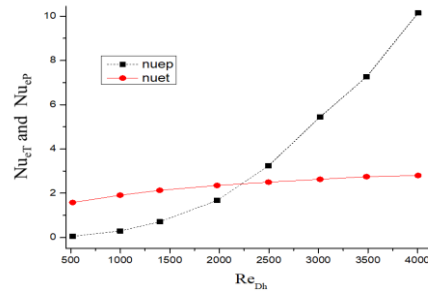


Figure 7. Variation of Nu_{eT} and Nu_{eP} with Re_{Dh}

4. Experimental equipment and results

4.1. Experimental platform

Set the equipment station as shown in Fig.8. Air enters NGVCP by a fan. The fan is a centrifugal blower with a power ranging 0–80W. The anemometer measures the maximum and average flow velocities of the air duct, and has a measurement accuracy of 0.1 m/s. The thermometer is integrated with the anemometer and has a measurement accuracy of 0.1°C. For temperature measurement, an *Omega* thermocouple with an SMPW plug is used, which has an accuracy of 0.75%. The channel composes the electric heating plate (80mm × 200mm) filling with foam copper. Resistance wire snakes through 12mm thick ceramic plate and arranges evenly in the electric heating plate. Outside wrappers are white sheet iron of 1mm thickness.

4.2. Characterization

To verify the correctness and accuracy of the experimental data, collect the experimental data after the working conditions are fully stable. When the channel is empty, it takes about 9 hours. When the porous media is filled in the channel, the time is about 7 hours.

In order to ensure air speed accurate measurement results and uniform distribution, it is necessary to set a straight section of no less than $5D$ (D represents the air duct diameter) in front of the anemometer and no less than $3D$ at the back, as shown in Fig.8. Section A connects the fan and anemometer. Section B is a 90mm ($>3D$) straight pipe section and a variable diameter pipe connected to the rectangular channel. Section C is a rectangular channel, and its size is consistent with the narrow gap channel. Section D is a narrow gap vertical channel test section formed by two electric heating plates. Section E is the same size as Section C to prevent backflow.

In order to reduce temperature measurement errors, measure the wall temperatures at different locations under different heat fluxes and different inlet velocities. First, use sealing device on test section and apply thermal grease evenly between the white iron sheet and the ceramic plate to reduce the contact thermal resistance. Set six temperature measurement points evenly on the electric heating plate to accurately obtain the mean wall temperature. Temperature measurement points horizontal spacing is 28.5mm and vertical spacing of 26mm , 27mm , and 27mm from bottom to top. Calibrate the temperature measurement system before the experiment in a constant temperature water tank. The relative error of the thermocouples remains within 0.5% , with most of them being less than 0.3% .

The volume of the solid skeleton of the porous material is calculated through Archimedes' buoyancy principle, and the volumetric porosity is obtained by the high precision hydrostatic balance, as shown in Fig.9. Each type of porous medium used in the experiment is evenly divided into ten equal parts and each part has a size of $40\text{mm} \times 40\text{mm} \times 4\text{mm}$. Then the average value is calculated to get the volumetric porosity of each porous media. It is important to evacuate the air bubbles inside the porous material to ensure accurate measurement of porosity.

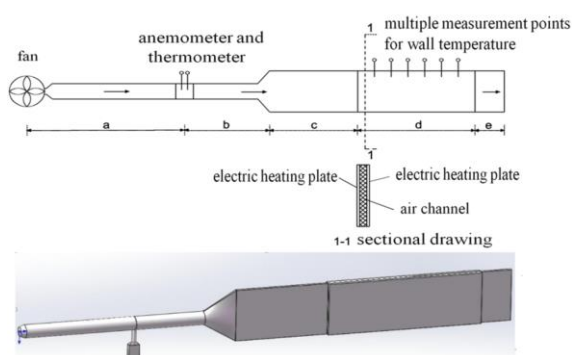


Figure 8. Experimental platform

Figure 9. Hydrostatic balance of measuring porosity

4.3. Results and discussion

The Fig.10 shows the wall temperature gradually increases along the flow direction initially, while there is slight decrease not far from the outlet. Because test section is connected to the downstream of non-heating air duct, and heat conduction causes the wall temperature decrease at the outlet. The wall temperature of channel filled with foam copper at the same point decreased significantly than that of empty channel, and the maximum decrease is 1.8°C . When air flows through the porous media channel, it is disturbed by the complex pore edges of the foam copper. The magnitude and direction of the air velocity constantly change, enhancing the turbulent effect. Moreover, the heat transfer area is greatly increased, which enhances heat transfer. Change gap width 8mm - 4mm and repeat experiment, the results are displayed in Fig.11. The maximum temperature

increases about 2.3°C, and the average temperature increases up to 1.8°C. When the inlet velocity is constant, the channel equivalent diameter decreases, so the convective heat transfer decreases and the wall temperature rise. This is mutually verified with the simulation results.

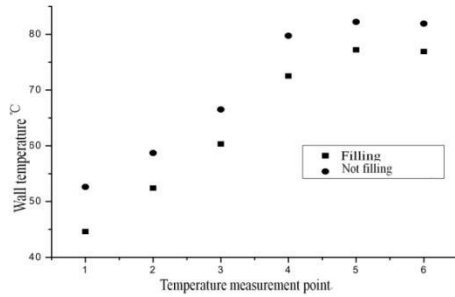


Figure 10. Wall temperature when filled and unfilled

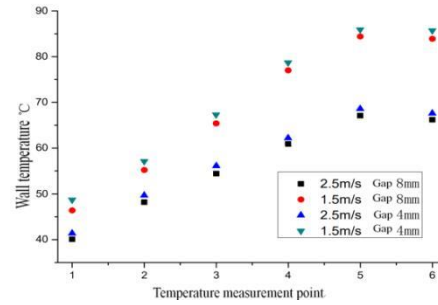


Figure 11. Wall temperature at different gap width

4.4. Experimental accuracy verification

Comparing the experimental data with the numerical simulation results of this study, it is obvious to see from Fig.12 that experimentation and simulation values are very close, and the average error is only 0.07. Comparing Re_{Dh} and Nu_{Dh} calculated this paper with the research results of Kurtbas [14] and Hutter [23], Fig.13 depicted all the trends are the same, but the Nu_{Dh} of this study is larger. First, heat loss because of ceramic insulation material in this study must be greater than that in previous experiments, but when calculating, the heat loss is calculated also according to 5%. Moreover, equivalent diameter of channel in this study is smaller. When the aspect ratio is small, Nu is larger.

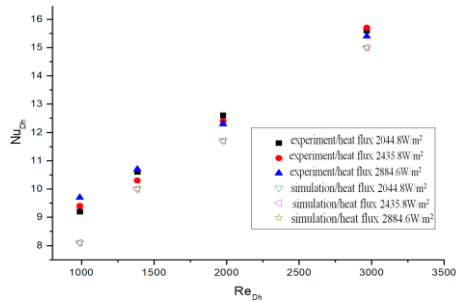


Figure 12. Comparison between experiment and simulation

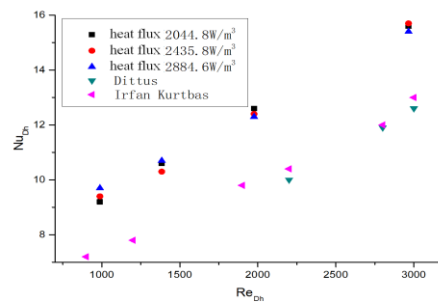


Figure 13. Comparison between experiment and before

5. Conclusion

5.1. Summary of the results

In summary, this study reports heat dissipation of NGVCP. Influence of channel geometric size, heat transfer parameters and porosity on the heat transfer mechanism in porous media was proposed.

According to theory research, derive the dimensionless velocity and dimensionless temperature and Nu number in porous media channel and empty channel, respectively.

Through numerical analysis, it is found that the velocity distribution and temperature distribution are more uniform due to the thinning of the boundary layer. When the air volume is constant,

convective heat transfer coefficient increases and then tends to stabilize as the aspect ratio increases. While when the flow velocity is constant, it lessens, but the Nu number based on equivalent diameter shows an increasing trend. When aspect ratio is 0.1, the convective heat transfer coefficient reaches its maximum. As the porosity increases, the convective heat transfer coefficient and Nu_{Dh} number both increase.

We fitted the criterion equations for resistance, heat transfer and exergy of NGVCP to explain the influence of porosity, Re number based on the equivalent diameter and channel width to height ratio on the heat transfer process. The relative error between simulation results and fitting results about f and Nu is almost within $\pm 10\%$ and $\pm 8\%$, respectively. For this study, the exergy critical Re_{Dh} number is 2147.5. Here, $Nu_{eT} = Nu_{ep} = 2.273$, and $Nu_e = 0$.

Set up an experimental platform and test the wall temperature and air velocity in the narrow vertical gap channel filling copper foam to verify the correctness of the simulation results. It is believed that this study can provide theoretical guidance for cooling design of high power devices.

5.2. Suggestions for further study

In this article, the heat dissipation mechanism of NGVCP is investigated. However, a special feature of porous media is the increase in resistance. For NGVCP, analysis of the resistance performance and testing of pressure drop are also required to be verified in real conditions, which could motivate future research. In addition, the conclusions of this study can be applied to further research on automotive battery packs or high density power electronic devices cooling.

Acknowledgements

This work received financial supports from the National Natural Science Foundation of China under Grant No. 52205535, China Postdoctoral Science Foundation - Tianjin Joint Support Program under Grant Number 2024T012TJ and Tianjin Vocational Institute innovation practice cultivation project. The authors thank Dr. Lingtao Weng from Tianjin University for technical support.

References

- [1] Bongole, K., *et al.*, Heat Transfer Characteristics of a Single Fracture with Different Fracture Surface Roughness Levels and Aperture Variations, *Journal of Porous Media*, 23 (2020), 5, pp. 445-463
- [2] El-Dabe, N., *et al.*, The Motion of a Non-Newtonian Nanofluid over a Semi-Infinite Moving Vertical Plate through Porous Medium with Heat and Mass Transfer, *Thermal Science*, 24 (2020), 2B, pp. 1311-1321
- [3] Hu, P., *et al.*, Effect of Interface Momentum Distribution on the Stability in a Porous-Fluid System, *Journal of Applied Fluid Mechanics*, 13 (2020), 3, pp. 1037-1046
- [4] Mahmoudi, Y., Constant Wall Heat Flux Boundary Condition in Micro-Channels Filled with Internal Heat Generation under Local Thermal Non-Equilibrium Condition, *International Journal of Heat and Mass Transfer*, 85 (2015), pp. 524-542

- [5] Ouyang, X., *et al.*, Thermal Boundary Conditions of Local Thermal Non-Equilibrium Model for Convection Heat Transfer in Porous Media, *International Journal of Heat and Mass Transfer*, 60 (2013), pp. 31-40
- [6] Dehghan, M., *et al.*, On the Thermally Developing Forced Convection through a Porous Material under the Local Thermal Non-Equilibrium Condition: An Analytical Study, *International Journal of Heat and Mass Transfer*, 92 (2016), pp. 815-823
- [7] Dehghan, M., *et al.*, Conjugate Heat Transfer inside Microchannels Filled with Porous Media: An Exact Solution, *Journal of Thermophysics and Heat Transfer*, 30 (2016), 4, pp. 814-824
- [8] Dehghan, M., *et al.*, Microchannels Enhanced by Porous Materials: Heat Transfer Enhancement or Pressure Drop Increment, *Energy Conversion and Management*, 110 (2016), pp. 22–32
- [9] Akbarzadeh, M., *et al.*, The Optimum Position of Porous Insert for a Double-Pipe Heat Exchanger Based on Entropy Generation and Thermal Analysis, *Journal of Thermal Analysis and Calorimetry*, 139 (2020), pp. 411–426
- [10] Zafari, M., *et al.*, Microtomography-Based Numerical Simulation of Fluid Flow and Heat Transfer in Open Cell Metal Foams, *Applied Thermal Engineering*, 80 (2015), pp. 347-354
- [11] Abu Shaban, N., *et al.*, Investigation of Transient and Steady Heat Transfer in Saturated Porous Medium Filled in a Vertical Cylinder with Thermal Dispersion and Radiation, *Thermal Science*, 26 (2022), 4A, pp. 3143-3155
- [12] Pamuk, M., Numerical Study of Heat Transfer in a Porous Medium of Steel Balls, *Thermal Science*, 23 (2019), 1, pp. 271-279
- [13] Bahmani, M., *et al.*, Numerical Study of the Porous Cavity with Different Square Size Vanes with a High Focus on Nusselt Number, *International Journal of Thermofluids*, 24 (2024), pp. 1-18
- [14] Kurtbas, I., *et al.*, Exergy Transfer in a Porous Rectangular Channel, *Energy*, 35 (2010), pp. 451-460
- [15] Sayyou, H., *et al.*, Natural Nanofluid Convection in Rectangular Porous Domains, *Thermal Science*, 28 (2024), 2A, pp. 929-939
- [16] Kuriyama, S., *et al.*, Study on Heat Transfer Characteristics of the One Side-Heated Vertical Channel with Inserted Porous Materials Applied as a Vessel Cooling System, *Nuclear Engineering & Technology*, 47 (2015), pp. 534-545
- [17] Chen, X., *et al.*, Conjugated Heat Transfer Analysis of a Foam Filled Double-Pipe Heat Exchanger for High-Temperature Application, *International Journal of Heat and Mass Transfer*, 134 (2019), pp. 1003-1013
- [18] Huisseune, H., *et al.*, Comparison of Metal Foam Heat Exchangers to a Finned Heat Exchanger for Low Reynolds Number Applications, *International Journal of Heat and Mass Transfer*, 89 (2015), pp. 1-9
- [19] Jalili, B., *et al.*, Investigation of the Unsteady MHD Fluid Flow and Heat Transfer through the Porous Medium Asymmetric Wavy Channel, *Case Studies in Thermal Engineering*, 61 (2024), pp. 1-19

- [20] Ahmadi Azar, A., *et al.*, Analytical Solution For MHD Nanofluid Flow over a Porous Wedge with Melting Heat Transfer, *Heliyon*, 10 (2024), pp. 1-20
- [21] Nield, D., Bejan, A., *Convection in Porous Media*, Springer, New York, United States, 2013
- [22] Dehghan, M., *et al.*, Combined Conduction-Convection-Radiation Heat Transfer of Slip Flow inside a Micro-Channel Filled with a Porous Material, *Transp Porous Med*, 108 (2015), pp. 413–436
- [23] Hutter, C., *et al.*, Heat Transfer in Metal Foams and Designed Porous Media, *Chemical Engineering Science*, 66 (2011), 17, pp. 3806–3814

Received: 12.10.2024.

Revised: 18.11.2024.

Accepted: 20.11.2024.